Progress In Electromagnetics Research M, Vol. 68, 99–107, 2018

A Low Phase-Noise SIW Reflection Oscillator with Hexagonal Resonator

Ziqiang Xu[1, *], Li Tan[1], Yuanxun Li[1], and Si Huang[2]

Abstract—A low phase noise reflection oscillator using a hexagonal substrate integrated waveguide (SIW) resonator is proposed in this paper. The hexagonal SIW resonator, which can combine flexibility of a rectangular cavity and performance of a circular cavity, is convenient for oscillator design. Since any of the six sides of a hexagonal resonator can be utilized for coupling, the oscillator configuration is flexible and adaptable. A simplified generalised phase noise condition and its optimization approach are proposed for the low-phase noise oscillator design. Furthermore, a 10.4 GHz oscillator prototype was designed, fabricated and measured to validate the proposed optimization approach. The measured results show that this oscillator provides 11.3 dBm output power and possesses low phase noise of −127.2 dBc/Hz at 1 MHz offset from 10.37 GHz carrier frequency, which is suitable for low-cost application in microwave and millimeter-wave band.

1. INTRODUCTION

The diversity of radio application, which causes strain on frequency resource and brings rapid development of novel millimeter-wave radar and wireless communication. Oscillator, as one of the core components, which has the performance of low phase-noise, high output frequency and great output power can fulfill stringent requirements in radar and communication system applications. Therefore, it is very significant to carry out researches on high performance and low phase-noise planar oscillators.

Phase-noise is one of the key parameters for oscillators design. Various ways have been implemented to enhance output power and reduce phase-noise of microwave oscillators. In recent years, substrate integrated waveguide (SIW) has not only a flat structure and easy integration compared with microstrip resonator, but also the traditional metal waveguide resonator's excellent advantages, such as low insertion loss, high Q-factor, high performance and high power capacity [1]. Thus, using a high Q-factor resonator such as SIW resonator as a frequency selective element is one of the most effective methods to realize low phase noise. In terms of mode, for instance, different resonators or cavities can provide a variety of modes to generate a large delay to reduce phase-noise. TE_{120} mode is applied in the feedback loop of the oscillator as a frequency stabilization element [2]. A quarter mode substrate integrated waveguide (QSIW) is used in oscillator and is stabilized in TE_{101} mode [3]. Oscillator is stabilized with TE_{210} differential mode of a single planar SIW rectangular resonator [4]. SIW dual-mode filter can degenerate two modes (TE_{102} and TE_{201}) to generate a large delay peak for improving the phase noise [5]. Meanwhile, different structures can be used to reduce volume and realize high Q-factor, such as half mode substrate integrated waveguide (HMSIW) [6] and quarter mode substrate integrated waveguide (QSIW) [3]. In addition, different materials and processes are utilized to improve integration and enhance Q-factor, including ferrite loaded substrate integrated waveguide (FLSIW) [7] and low temperature co-fired ceramic (LTCC) [8]. Different resonators have been used for oscillator design,

---

Received 12 March 2018, Accepted 25 April 2018, Scheduled 7 May 2018

[*] Corresponding author: Ziqiang Xu (nanterxu@uestc.edu.cn).

[1] School of Materials and Energy, University of Electronic Science and Technology of China, China. [2] Electrical Engineering, University of Arkansas, USA.

for instance, rectangle resonator [9, 10], circular resonator [11–13], complementary coupled resonator (CRR) [14], fourth-degree cross coupled band-pass SIW filter [15], active resonator [16–18], and split ring resonator [19, 20].

In this paper, a reflection oscillator with low phase noise using a hexagonal SIW resonator is presented. The hexagonal resonator not only possesses similar resonant characteristics of circular SIW one, but also possesses a higher Q-factor than rectangle one. Meanwhile, it has the characteristics of stable structure, which can be easy for fabrication. Therefore, the hexagonal SIW resonator can get a better performance to design oscillators. By combining features of microstrip line and hexagonal SIW resonator, the output frequency of oscillator can be adjusted and modified conveniently. A reflection oscillator of 10.4 GHz is designed and implemented to validate the proposed design ultimately. The measured results are also given and discussed.

2. OSCILLATOR ANALYSES AND DESIGN

An SIW resonator consists of six separate rows of metallized holes, which is integrated in a dielectric substrate and used to form a dielectric filled synthesized hexagonal resonator. The configuration of the hexagonal SIW resonator and its electric field distributions are illustrated in Figure 1. Here, the initial dimensions of the hexagonal resonator can be determined by the modified formula as follows [21]:

$$W_{\text{siw}} = \frac{c}{\sqrt{\varepsilon_r}} \cdot \frac{u}{2\pi f_0} \tag{1}$$

where u is the modified root coefficient based on Bessel function, and the value is 2.75, c the speed of light in free space, ε_r the relative permittivity of dielectric substrate, and f_0 the fundamental resonant frequency. The equilateral length of the hexagonal resonator is W_{siw}; the diameter of metallized hole is d; the center of two adjacent metallized holes is p.

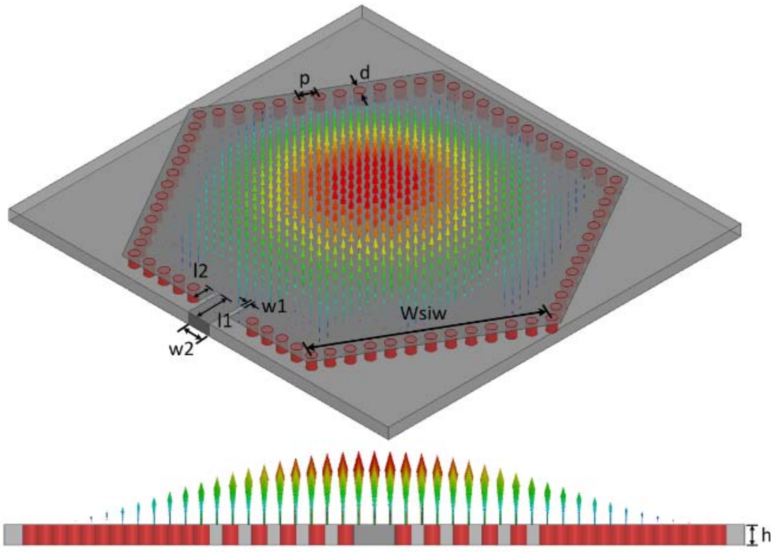

Figure 1. Configuration and E-field distributions of the SIW hexagonal resonator.

To obtain the final geometrical parameters, two variables, namely $w1$ and $l1$, are selected for explanation. In Figure 2, the resonance frequency increases with decrement of $w1$ and $l1$, respectively. The geometrical parameters of the SIW hexagonal resonator are listed in Table 1. The SIW hexagonal resonator is validated on a substrate using Rogers RT/Duroid 5880 with relative dielectric constant of $\varepsilon_r = 2.2$, loss tangent of 0.0009, and thickness of 0.508 mm.

Figure 3 shows a photograph of fabrication of the SIW hexagonal resonator along with S_{11} parameter with Driven Mode by HFSS (High Frequency Structure Simulator). The result shows that

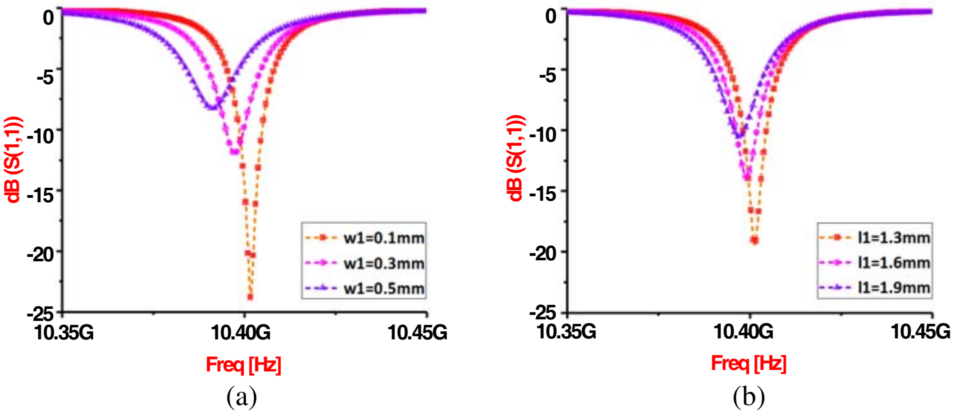

Figure 2. Resonant frequency with the change of $w1$ and $l1$: (a) resonance frequency with the change of $w1$ (b) resonance frequency with the change of $l1$.

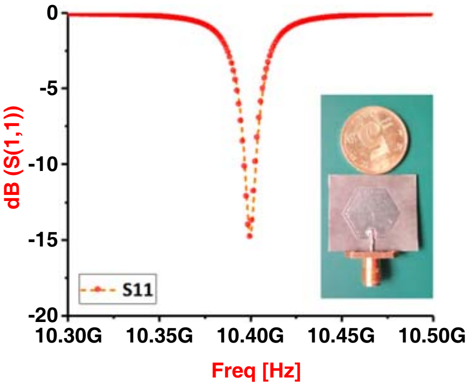

Figure 3. Photograph of fabrication SIW hexagonal resonator along with the S_{11}.

Table 1. The final dimensions of the SIW hexagonal resonator (unit: mm).

$Wsiw$	h	d	p	$l1$	$l2$	$w1$	$w2$
8.4	0.508	0.4	0.7	1.5	1	0.2	1

resonant frequency is about 10.4 GHz. Loaded Q-factor of 303.6 for the SIW resonator can be estimated from the formula.

$$Q = \frac{f_0}{\Delta f_{-3\,\mathrm{dB}}} \tag{2}$$

where f_0 is the fundamental resonant frequency, $\Delta f_{-3\mathrm{dB}}$ the frequency difference between two frequencies, and their corresponding S_{11} value is 3 dB. The unloaded Q-factor can also be obtained by eigenmode with HFSS, and the unloaded Q-factor is 1154.8.

In order to prevent the crosstalk of high frequency signal and DC signal, it is necessary to design a high frequency choke circuit. Its role is equivalent to a band-stop filter. The sector bias circuit with angle A and radius lr is designed to change the stopband of high frequency choke circuit. Figures 4(a) and (b) display the simulation with variation of radius and angle, respectively. Through the simulation we can comprehend that radius lr is a significant factor and has impact on center frequency. Similarly, with the increase of radius, center frequency decreases, which means that angle A has a certain influence on the center frequency. Therefore, the radius can be utilized as a wide range of tuning and the angle as a small one. It can be understood that there is on obstacle of signal transmission at the low frequency,

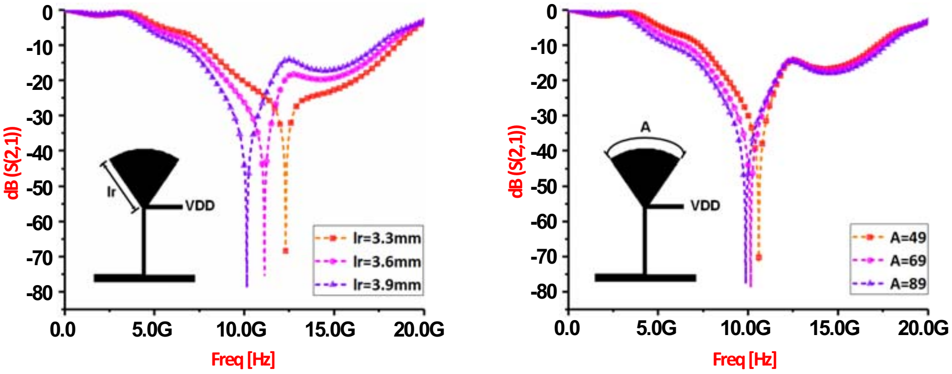

(a) (b)

Figure 4. Center frequency with the change of angle and radius: (a) center frequency with the change of angle and (b) center frequency with the change of radius.

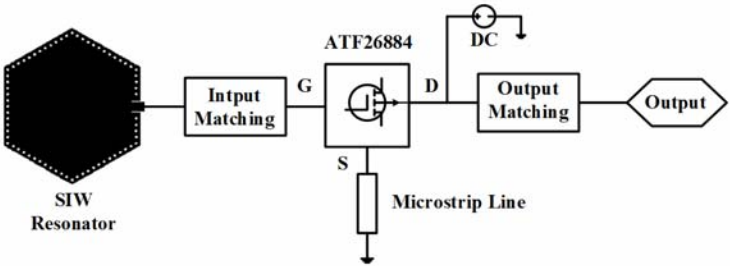

Figure 5. Schematic diagram of the SIW reflection oscillator.

and the values of S_{21} are less than 30 dB near 10.4 GHz. Thus, it can effectively prevent the crosstalk between generated signal and DC signal. Finally, the final selected values are $A = 69^\circ$, $lr = 3.3\,\mathrm{mm}$. The topology of the above-mentioned SIW reflection oscillator is shown in Figure 5.

The amplifier used here is the GaAs FET-ATF26884, from Agilent. The source connects the microstrip line and makes the amplifier unstable. In order to ensure that the amplifier is unstable, the method adds a grounded microstrip line to the grid electrode and uses StabFact to control and adjust the length of grounded microstrip line repeatedly. In this process, $|K| < 1$ and $S_{11} < 1$ should be ensured. Finally, it can observe the instability of coefficient K by ADS (Advanced Design system) in Figure 6.

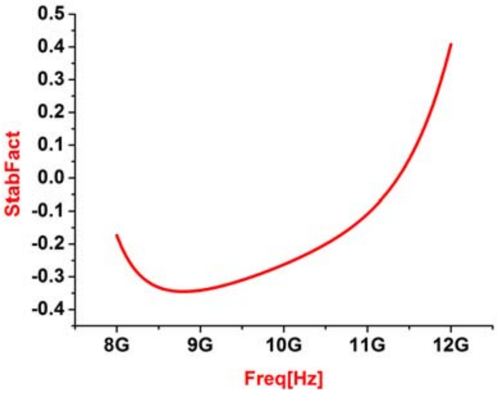

Figure 6. The results of instability.

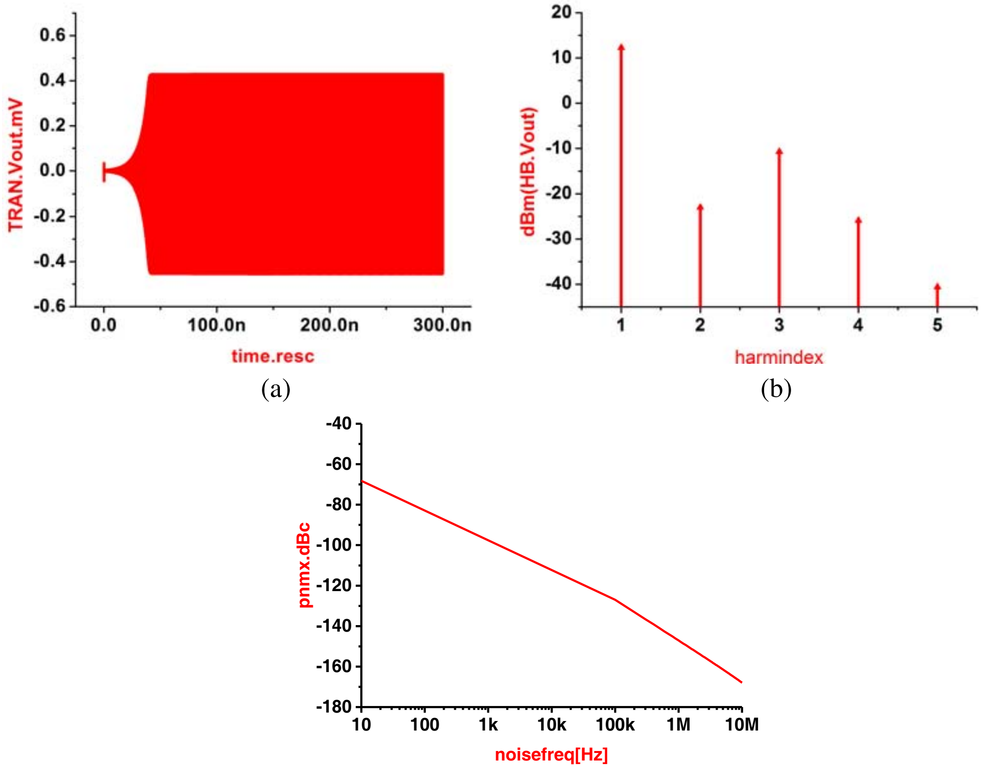

(a) (b) (c)

Figure 7. Layout-schematic simulation of SIW reflection oscillator: (a) transient analysis, (b) harmonic power, and (c) phase-noise.

Layout-schematic simulation of reflection type oscillator is shown in Figure 7. The TRANSIENT simulation tool is used for TRANSIENT analyses, which can obtain a stable output voltage of output port. The Harmonic Balance (HB) tool is used for Harmonic simulation and obtains the fundamental wave power of 12.3 dBm. The second-harmonic power is −23 dBm, and the phase noise is −147.1 dBc/Hz@1 MHz.

3. FABRICATION AND EXPERIMENTAL RESULTS

To validate the proposed optimization process, an experimental 10.4 GHz SIW reflection oscillator was fabricated. The final geometrical parameters chosen for the design of the reflection oscillator are listed in Table 2. For convenience, we choose the bias voltage and current of VDS = 4 V, VGS = 0 V and IDS = 43 mA, respectively. The layout of the hexagonal SIW reflection oscillator is illustrated in Figure 8. Besides, Figure 9 displays a photograph of the fabrication SIW reflection oscillator.

The proposed SIW reflection oscillator is fabricated on a Rogers RT/Duroid 5880 substrate with the dielectric constant of 2.2 and thickness of 0.508 mm. Agilent N9010A spectrum analyzer is used to

Table 2. The final dimension of the reflection oscillator (unit: mm, angle A: degree).

$l3$	$l4$	$l5$	$l6$	$l7$	$l8$	$l9$	$l10$	$l11$
10.3	7	8.3	2	2.6	8.6	5.5	2.7	2
$l12$	$l13$	lr	$w1$	$w3$	$w4$	$w5$	$w6$	A
5.5	2.5	3.3	1	0.2	0.08	1	2	69

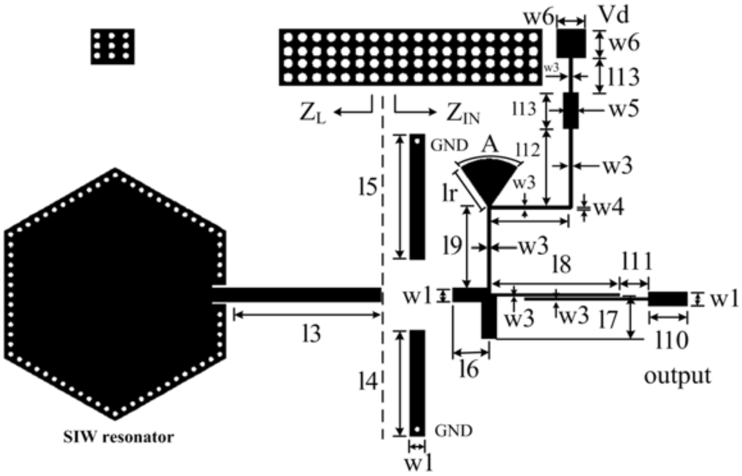

Figure 8. The layout of the SIW reflection oscillator.

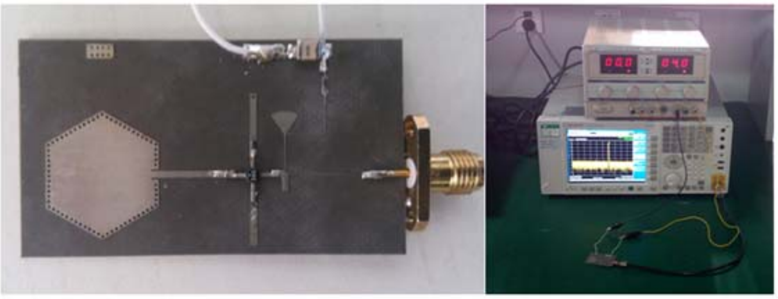

Figure 9. Photographs of fabrication SIW reflection oscillator and measurement environment.

measure the output spectrum of the SIW reflection oscillator in terms of output spectrum performance parameters including oscillation frequency and phase noise at the fundamental wave port.

The proposed reflection oscillator's output spectra at the fundamental and second frequencies are shown in Figures 10(a) and (b). The phase noise of oscillator is given in Figure 10(c). The red and black curves represent measured curve and fitting curve, respectively. The output frequency is 10.37 GHz, and the power output level is more than 11.3 dBm. It is shown that the circuits have a good match. The second harmonic power level is −18 dBm. It is illustrated that this oscillator obtains an excellent anti-interference performance. The phase noise achieves −127.2 dBc/Hz@1 MHz, and its curve is smooth. Thus, the proposed SIW reflection oscillator exhibits good features which can be suitable for microwave application.

In comparison with the performance of the oscillator, now one of the prevalent approaches adopts FoM (Figure of Merit) [22] to measure its performance. The computational formula is given as follows:

$$FoM = L\left(\Delta f\right) - 20\log\left(\frac{f_0}{\Delta f}\right) + 10\log\left(\frac{P_{DC}}{1\,\mathrm{mW}}\right) \tag{3}$$

where $L(\Delta f)$ is the noise of offset frequency. Because the measured noise is -127.2 dBc/Hz@1 MHz, $L(\Delta f) = -127.2$, and Δf is the size of the noise of offset frequency, thus, $\Delta f = 1\,\mathrm{MHz}$. f_0 is center of frequency, $f_0 = 10.37\,\mathrm{GHz}$. P_{DC} is the power supply, $P_{DC} = 4\,\mathrm{V} * 20\,\mathrm{mA} = 80\,\mathrm{mW}$. Thus, the calculated value of FoM is about −189 dBc/Hz. FoM is usually a negative value, and when it gets smaller, its performance gets better. It can refer to the relevant literature and compare FoM with those of other oscillators. The conclusion shows as in Table 3. It is well known that the FoM value of an excellent oscillator should be less than −160. The proposed oscillator's FoM value is −189. Thus, it validates that the proposed oscillator exhibits good performance compared with that in Table 3.

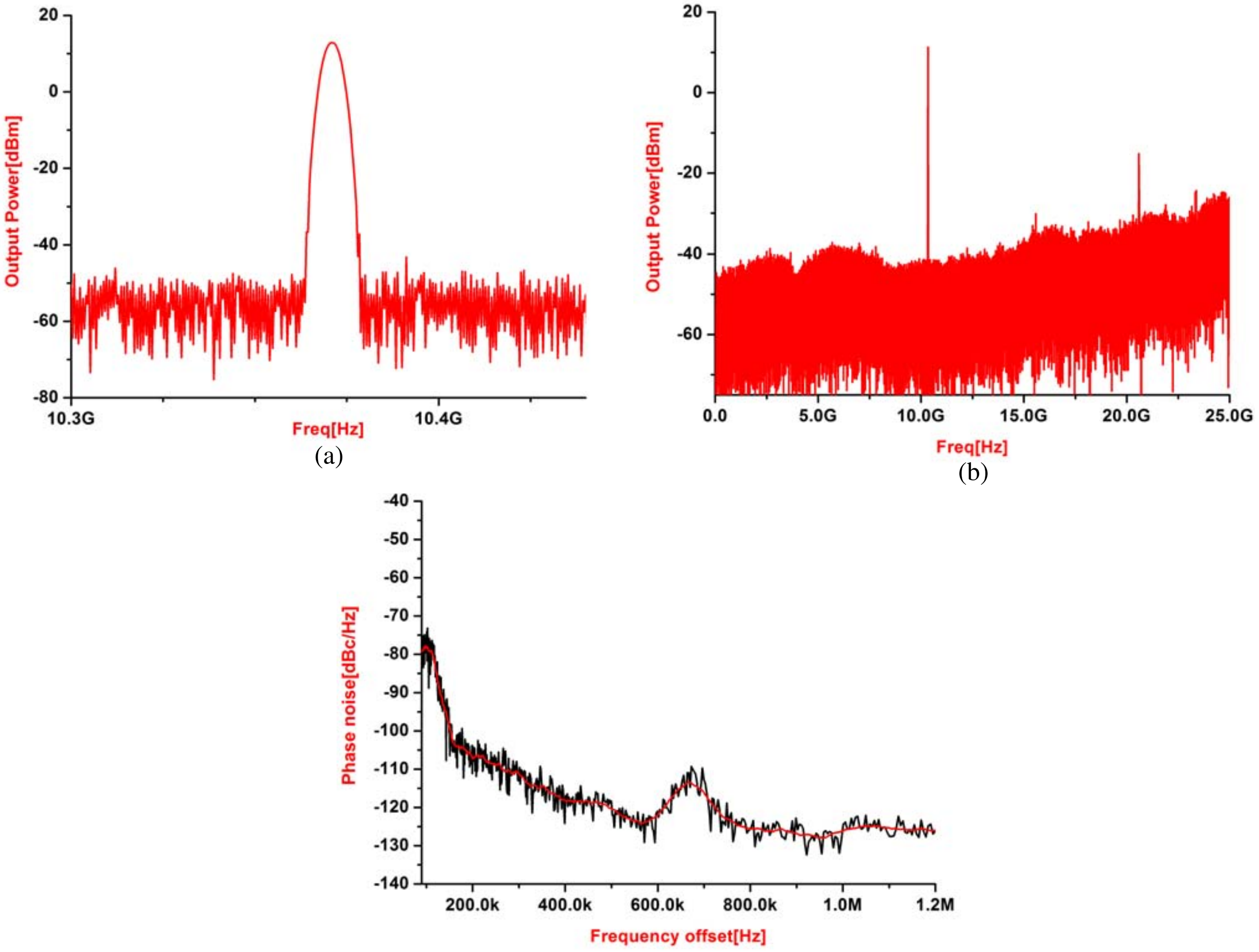

(a) (b) (c)

Figure 10. Measurement results of the SIW reflection oscillator: (a) output power spectrum (b) harmonic power spectrum (c) phase-noise.

Table 3. Comparison between published SIW oscillators and the SIW oscillator in this article.

Reference	**Output frequency (GHz)**	**L@100 KHz (dBc/Hz)**	**L@1 MHz (dBc/Hz)**	**Output power (dBm)**	**FoM**
[11]	11.45	−109.2	−130.5	2.01	−192.8
[13]	11.57	117.3	135.5	−2.3	206.2
[23]	9.5	−88	−117	7.5	−184
[24]	29.5	−70.5	−105.7	−14.7	−182.4
[25]	2.675	−105.5	−118.2	5.33	−171.8
[26]	5.09	−121.6	−115.2	8	−174.1
[27]	10.98	−121.6	−143.3	−1.8	−211.5
This work	10.37	−81.7	−127.2	11.3	−189

4. CONCLUSION

In this paper, a low phase-noise reflection oscillator with a hexagonal SIW resonator is presented. Since any of the six sides of a hexagonal SIW resonator can be used for coupling, the oscillator configuration is flexible and adaptable. A 10.4 GHz prototype was designed, fabricated and measured. From experimental data, it can be found that the oscillator's output center frequency at the fundamental-wave output port is 10.37 GHz, and the phase noise is -127.2 dBc/Hz@1 MHz. This oscillator also provides 11.3 dBm output power. Besides, the structure of the oscillator possesses some advantages including easy integration, small volume, light weight, good frequency stability, as well as low phase-noise. This SIW reflection oscillator exhibits an excellent performance, which is suitable for the application of microwave and millimeter-wave engineering.

ACKNOWLEDGMENT

This work was supported by the National Natural Science Foundation of China (Grant No.: 61301052), Fundamental Research Funds for the Central Universities of China (Grant Nos. ZYGX2015J095 and ZYGX2016J0145), Chengdu electric vehicle industry cluster innovation project (Grant No. 2017-XT00-00002-GX), and Sichuan Science and Technology Program (Grant Nos. 2018GZ0010, 2016GZ0025, 2017GZ0102, 2017GZ0106, 2017GZ0143, and 2017GZ0020).

REFERENCES

1. Bozzi, M., A. Georgiadis, and K. Wu, "Review of substrate-integrated waveguide circuits and antennas," *IET Microwaves Antennas & Propagation*, Vol. 5, No. 8, 909–920, 2011.
2. Yang, Z., B. Luo, J. Dong, et al., "X-band low phase noise loop oscillator with differential outputs," *Electronics Letters*, Vol. 51, No. 13, 1005–1007, 2015.
3. Yang, Z., B. Luo, J. Dong, et al., "Low phase noise oscillator based on quarter mode substrate integrated waveguide technique," *IEICE Electronics Express*, Vol. 12, No. 6, 20150046–20150046, 2015.
4. Yang, N., C. Caloz, and K. Wu, "TE_{210} mode balanced oscillator using substrate integrated waveguide resonator," *IET Microwaves Antennas & Propagation*, Vol. 5, No. 10, 1188–1194, 2011.
5. Yang, Z., B. Luo, J. Dong, et al., "X-band low-phase noise oscillator employing substrate integrated waveguide dual-mode filter," *Electronics Letters*, Vol. 51, No. 6, 494–495, 2015.
6. Zhuang, C., J. Xu, F. Yu, et al., "Design of half mode substrate integrated waveguide Gunn oscillator," *IEEE Transactions on Components Packaging & Manufacturing Technology*, Vol. 1, No. 11, 1790–1794, 2011.
7. Adhikari, S., A. Ghiotto, and K. Wu, "Low-cost frequency modulated ferrite loaded SIW oscillator for high-power microwave transmitter," *IEEE Microwave Symposium Digest*, 1–3, 2014.
8. Dancila, D., X. Rottenberg, H. A. C. Tilmans, et al., "Low phase noise oscillator at 60 GHz stabilized by a substrate integrated cavity resonator in LTCC," *IEEE Microwave & Wireless Components Letters*, Vol. 24, No. 12, 887–889, 2014.
9. Chen, Z., W. Hong, and J. X. Chen, "High-Q planar active resonator based on substrate integrated waveguide technique," *Electronics Letters*, Vol. 48, No. 10, 575–577, 2012.
10. Liu, Y., X. H. Tang, and T. Wu, "SIW-based low phase-noise millimeter-wave planar dual-port voltage-controlled oscillator," *Journal of Electromagnetic Waves and Applications*, Vol. 26, Nos. 8–9, 1059–1069, 2012.
11. Li, Z., Y. Liu, and J. Bao, "A phase noise reduction method in microwave oscillator using a high-Q transmission line loaded with active SIW resonator," *Microwave & Optical Technology Letters*, Vol. 58, No. 1, 221–225, 2016.
12. Duong, T. V., W. Hong, V. H. Tran, et al., "An alternative technique to minimize the phase noise of X-band oscillators using improved group delay SIW filters," *IEEE Microwave & Wireless Components Letters*, Vol. 27, No. 2, 153–155, 2017.

13. Huang, W., J. Zhou, and P. Chen, "An X-band low phase noise free-running oscillator using substrate integrated waveguide dual-mode bandpass filter with circular cavity," *IEEE Microwave & Wireless Components Letters*, Vol. 25, No. 1, 40–42, 2015.
14. Wu, C. T. M., T. Itoh, A. K. Poddar, et al., "Active complementary coupled resonator for low phase noise X-band oscillator," *IEEE European Frequency and Time Forum*, 356–359, 2015.
15. Lin, J., H. Zhang, W. Kang, et al., "Design of low phase noise substrate integrated waveguide oscillator based on complexquality factor (Qsc)," *IEEE International Conference on Ubiquitous Wireless Broadband*, 1–3, 2016.
16. Chen, Z., W. Hong, J. X. Chen, et al., "Low-phase noise oscillator utilising high-Q active resonator based on substrate integrated waveguide technique," *IET Microwaves Antennas & Propagation*, Vol. 8, No. 3, 137–144, 2013.
17. Stornelli, V., L. Pantoli, and G. Leuzzi, "Active resonator for low-phase-noise tunable oscillators," *Microwave & Optical Technology Letters*, Vol. 58, No. 5, 1032–1035, 2016.
18. Nick, M. and A. Mortazawi, "Low phase-noise planar oscillators based on low-noise active resonators," *IEEE Transactions on Microwave Theory & Techniques*, Vol. 58, No. 5, 1133–1139, 2010.
19. Hamidkhani, M. and F. Mohajeri, "A low phase noise microwave oscillator based on a high Q SIW cavity CSRR band-pass filter," *Journal of Electromagnetic Waves and Applications*, Vol. 30, No. 16, 2077–2087, 2016.
20. Park, W. Y. and S. Lim, "A low phase-noise microwave oscillator using a substrate integrated waveguide resonator based on complementary split ring resonator," *IEEE Microwave Conference Proceedings*, 371–374, 2011.
21. Xu, Z. Q., Y. Shi, P. Wang, et al., "Substrate integrated waveguide (SIW) filter with hexagonal resonator," *Journal of Electromagnetic Waves and Applications*, Vol. 26, Nos. 11–12, 1521–1527, 2012.
22. Li, Z., Y. Liu, and J. Bao, "A K-band push–push oscillator employing differential transmission line loaded with SIW cavity operated in TM_{110} mode," *Microwave & Optical Technology Letters*, Vol. 58, No. 5, 1217–1221, 2016.
23. He, F. F., K. Wu, W. Hong, et al., "A low phase-noise VCO using an electronically tunable substrate integrated waveguide resonator," *IEEE Transactions on Microwave Theory & Techniques*, Vol. 58, No. 12, 3452–3458, 2010.
24. Georgiadis, A., S. Via, A. Collado, et al., "Push-push oscillator design based on a substrate integrated waveguide (SIW) resonator," *IEEE European Microwave Conference, 2009, EuMC 2009*, 1231–1234, 2009.
25. Dong, Y. and T. Itoh, "A dual-band oscillator with reconfigurable cavity-backed complementary split-ring resonator," *IEEE Microwave Symposium Digest*, 1–3, 2012.
26. Wu, C. T. M., T. Itoh, A. K. Poddar, et al., "A C-band tunable oscillator based on complementary coupled resonator using substrate integrated waveguide cavity," *IEEE Microwave Conference*, 715–718, 2014.
27. Zhang, R., J. Zhou, Z. Yu, and B. Yang, "A low phase noise feedback oscillator based on SIW bandpass response power divider," *IEEE Microwave and Wireless Components Letters*, Vol. 28, No. 2, 153–155, Feb. 2018.